Modeling and Simulation of an Oxygen-Blown Bubbling Fluidized Bed Gasifier using the Computational Particle-Fluid Dynamics (CPFD) Approach

A. Di Nardo[†], G. Calchetti, S. Stendardo

ENEA, Italian National Agency for New Technologies Energy and Sustainable Economic Development, Rome, via Anguillarese 301, 00123, Italy

†*Corresponding Author Email: antonio.dinardo@enea.it*

ABSTRACT

Fluidized beds are conventional components of many industrial processes, such as coal gasification for energy generation and syngas production. Numerical simulations help to properly design and understand the complex multiphase flows occurring in these reactors. Two modeling approaches are usually adopted to simulate multiphase flows: the two fluids Eulerian-Eulerian model and the continuous/discrete Eulerian-Lagrangian model. Since fluidized beds account for an extremely large number of particles, tracking each of them could not assure to get results within a reasonable computational time. The Computational Particle-Fluid Dynamics (CPFD) approach, which belongs to the Eulerian-Lagrangian models class, groups together particles with similar key parameters (e.g. composition, size) into computational units (parcels). Parcel collisions are modeled by an isotropic solid stress function, depending on solid volume fraction. In this paper, the bubbling fluidized bed (BFB) upstream gasifier of the EU research infrastructure ZECOMIX (Zero Emissions of Carbon with Mixed technologies) has been simulated using a CPFD approach via Barracuda® software. The effect of different fluidizing agent injection strategies on bed bubbling and mixing, for non-reacting cases, has been studied. The numerical results for a reacting case have been compared to the available experimental data, gathered during the coal gasification campaign. The model has proved to be very useful in the choice of the more efficient injection configuration that assures a more effective contact of the gas with the solid bed and a good bubbling fluidization regime, together with a satisfactory prediction of the outlet gas composition. The numerical approach has turned out to be robust and time-saving and allowed to dramatically reduce the computational cost with respect the classical two fluids Eulerian-Eulerian models.

Keywords: Fluidized bed gasifier; CPFD method; Multiphase flows.

NOMENCLATURE

A_o	pre-exponential factor	Re	Reynold's number
A_p	particle acceleration	r_p	particle radius
C	smagorinsky coefficient	Sc	Schmidt number
C_D	drag coefficient	S_h	energy exchange between solid and gas
$C_{p,i}$	constant press. specific heat for species i	T_g	gas temperature
C_V	specific constant volume heat	T_p	particle temperature
D	turbulent mass diffusion rate	u_g	gas velocity
D_p	drag function	u_p	particle velocity
E	activation energy	$\bar{u}_p$	local mass averaged particle velocity
E_0	activation energy constant	x_s	particle trajectory coordinates
F	rate of momentum exchange	$Y_{g,i}$	species mass fraction
f_D	particle distribution func. for part. vel.	$\delta\dot{m}_{i,chem}$	net production rate of species
f_p	particle distribution function	$\delta\dot{m}_p$	gas mass production rate per volume
g	gravity acceleration	ε_{cp}	particle volume fraction close pack
h_g	gas enthalpy	ε_p	particle volume fraction
h_i	species enthalpy	ε_g	gas volume fraction

h_p	particle enthalpy	ε_p	particle volume fraction
k	reaction rate	λ_g	thermal conductivity
MW_i	molecular weight of gas species i	μ	shear viscosity
m_p	particle mass	μ_t	sub grid turbulent viscosity
Nu_g	Nusselt number	ρ_g	gas density
p, p_g	gas pressure	ρ_p	particle density
P_p	constant	τ_g	stress tensor
$\dot{Q}$	energy source per unit volume	τ_p	contact normal stress
q	gas heat flux	τ_D	particle collision damping time
$\dot{q}_D$	enthalpy diffusion term	Φ	viscous dissipation
R	universal gas constant		

1. INTRODUCTION

ZECOMIX (Zero Emissions of Carbon with Mixed technologies) is a European Research Infrastructure (ww w.meril.eu) managed by the Italian National Agency for the New Technologies, the Energy and the sustainable economic development (ENEA). It has been conceived to study decarbonisation process for producing electricity and hydrogen from conventional fuels (methane and coal). Coal gasification, steam methane reforming (SMR), clean-up of syngas, calcium looping (CaL) cycle for CO_2 capture and hydrogen combustion in a gas micro-turbine, are the main processes that can be thoroughly investigated by means of experimental and numerical activities. In particular, this paper is focused on the modeling and simulation of the gasification process. Particularly, the numerical results have been validated with experimental results gathered during coal gasification tests.

Fluidized bed technology plays an important role in many industrial processes (e.g. combustion and coal gasification) for energy generation and syngas production. In fluidized bed gasifier, coal particles are held in suspension by oxygen (or air) and steam flow, having the dual function of oxidizer and fluidizing agent. An intimate mixing between the solid particles and the gaseous mixture improves mass and heat transfer among the two phases. The gas bubbles formation, rising through the mass of the bed, also promotes and improves mixing of gas and solid materials in the bed.

Two types of modeling approaches are possible for multiphase flows to describe gas-solid interactions: a continuous approach for both phases, known as Eulerian-Eulerian model and a continuous/discrete approach known as Eulerian-Lagrangian model (Wang 2009, Wang *et al.* 2013, Lettieri and Mazzei 2009, Gidapow 1994, Gidapow *et al.* 2004, Deen *et al.* 2007). In the Eulerian-Eulerian model, the solid phase is treated as a pseudo-fluid. The conservation equations for both phases are derived and correlated by constituent relationships obtained from empirical information and/or kinetic theory. The Eulerian-Eulerian model has historically been used in the simulation of multiphase flows with some considerable limitations regarding, for example, the physical modeling of gas-particle, particle-particle and particle-wall interactions. Furthermore, equations for each particle dimensions must be solved to take into account the size distribution of the solid phase.

In the Eulerian-Lagrangian model, the gas phase is treated as a continuous fluid, by solving Navier-Stokes equations, while the solid phase is treated as a particle-dispersed phase and the particle trajectories are calculated taking into account particle-fluid interactions, such as turbulence, heat, mass and momentum exchanges. This approach presents, however, some limitations. In particular, it is assumed that the dispersed phase is sufficiently diluted so that particle-particle interactions are negligible and the volume of the solid phase is much lower than the volume of the continuous phase. Usually, the volume fraction should be less than 10-12 %, while the mass may also exceed this limit. The environment of a fluidized bed gasifier may deviate much from these hypotheses.

The CPFD approach (Snider and Banerjee 2010, Snider *et al.* 2011, O'Rourke *et al.* 2009, 2010), based on the MP-PIC (multiphase-particle-in-cell) method (Andrews and O'Rourke 1996, Snider 2001) is a Eulerian-Lagrangian model developed to simulate flows with high particles load. In particular, it introduces the concept of computational particles, called parcels, identified as a set of physical particles which have similar key parameters, as composition and size. As a consequence parcel represents a numerical approximation of the solid phase, similar to the concept of control volume used in CFD calculations, where fluid properties are considered constant. In this way it is possible to model systems with a high number of particles with a reasonable computational cost, since collisions are not directly calculated but modeled as a spatial gradient calculated on the Eulerian grid, by an isotropic solid stress function, depending on solid volume fraction, and then interpolated back on the discrete particles. The two phases are completely coupled in terms of mass and energy interchange.

Liang *et al.* (2014) simulated a bubbling fluidized bed with the CPFD method and compared the results with experimental data available in the literature. They found that the model is able to better predict solid velocity profiles than a model based on the Eulerian-Eulerian approach. Some open issues however still remained about bubbles evolution. Thapa *et al.* (2014) modeled a bubbling fluidized biomass gasifier with the CPFD approach, focusing in particular on reaction kinetics. Simulation results matched quite well the experimental data with regards to the syngas composition. Thapa *et al.* (2016) carried out an

optimization study of a circulating fluidized bed using the CPFD method and the results were validated against experimental results. Particularly, they found a good agreement between pressure drop and solid circulation rate with respect experimental data. Kraft *et al.* (2016) used the CPFD model to optimize a 50 MW bubbling fluidized bed biomass combustion chamber. The model successfully predicted temperature distribution and deposits on the furnace walls due to ash melting. Liu *et al.* (2015) studied a 3D full-loop fluidized bed biomass gasifier using the CPFD approach. The numerical results in terms of temperature profiles and output gas composition matched very well the experimental measurements. Karimipour *et al.* (2012) investigated the capability of the CPFD method to simulate bubbling fluidized bed, verifying that the model was able to better capture bubbles properties when compared to the results obtained by means of Eulerian-Eulerian approach.

The aim of the work is to study the upstream gasifier of the ZECOMIX plant using Barracuda® software, which is based on the CPFD approach. The study is divided into two parts. In the first section, the fluidization of the non-reacting olivine-coal particles bed is analyzed for different gas mass flow rate and different gas injection configurations. In a second section, a reacting model is used to simulate the syngas output, which is compared to the gasifier outlet composition experimental data, the only available at the moment. The CPFD method can take the advantage of Graphics Processing Units (GPUs) to parallelize particles computation. The simulations have been carried out on a ENEA CRESCO® 2 CPU quad-core Intel® Xeon® E5620 machine, equipped with a NVIDIA GPU TESLA K40, for 2880 CUDA cores, 1.43 Teraflops of double precision and 4.29 Teraflops of single precision peak performance.

2. GOVERNING EQUATIONS

The CPFD approach is based on the finite volume method. Scalars and momentum equations are calculated on a staggered grid. Turbulence is modeled by the Large Eddy Simulation (LES) model and the sub-grid viscosity is calculated according to the Smagorinsky model (Smagorinsky 1963). Pressure, velocity and density are coupled by a pressure equation, directly derived from mass conservation and the ideal gas equation of state is used for the pressure–density dependency. While other models calculate particles collisions using a spring-damper model and direct particle contact, the MP-PIC method models collisions by the particle normal stress function and makes use of spatial gradients, calculated on the Eulerian grid and then interpolated to discrete particles, treating particles as a continuum. The particle stress is derived from the particle volume fraction calculated from the particle volume mapped to the grid. The modified continuum particle stress model of Harris and Crighton (1994) has been modified in the denominator of Eq. (13) to prevent singularity at the close pack (is on the order of 10^{-7}). Particles

are assumed to have inner uniform temperature and the heat release due to chemical reactions does not contribute to particle energy balance. The basic governing equations for the gas and particles are reported in the following. For more details see Snider (2001), Snider and Banerjee (2010), Snider *et al.* (2011).

Fluid mass conservation equation

$$\frac{\partial(\varepsilon_g \rho_g)}{\partial t} + \nabla(\varepsilon_g \rho_g \boldsymbol{u}_g) = \delta \dot{m}_p$$

(1)

Fluid momentum equation

$$\frac{\partial(\varepsilon_g \rho_g \boldsymbol{u}_g)}{\partial t} + \nabla(\varepsilon_g \rho_g \boldsymbol{u}_g \boldsymbol{u}_g) =$$
$$-\nabla p + \boldsymbol{F} + \varepsilon_g \rho_g \boldsymbol{g} + \nabla \varepsilon_g \tau_g$$

(2)

Stress tensor

$$\tau_{g,i,j} = \mu \left(\frac{\partial u_i}{\partial x_j} + \frac{\partial u_j}{\partial x_i} \right) + \frac{2}{3} \mu \delta_{ij} \frac{\partial u_k}{\partial x_k}$$

(3)

Large Eddy Simulation unresolved sub grid turbulent viscosity

$$\mu_t = C \rho_g \Delta^2 \sqrt{\left(\frac{\partial u_i}{\partial x_j} + \frac{\partial u_j}{\partial x_i} \right)^2}$$

(4)

Fluid energy conservation equation

$$\frac{\partial(\varepsilon_g \rho_g \boldsymbol{h}_g)}{\partial t} + \nabla \cdot (\varepsilon_g \rho_g h_g \boldsymbol{u}_g) =$$
$$\varepsilon_g \left(\frac{\partial p}{\partial t} + \boldsymbol{u}_g \cdot \nabla p \right) + \Phi - \nabla \cdot (\varepsilon_g \boldsymbol{q}) + \dot{Q} + S_h + \dot{q_D}$$

(5)

Fluid species transport equation

$$\frac{\partial(\varepsilon_g \rho_g Y_{g,i})}{\partial t} + \nabla(\varepsilon_g \rho_g Y_{g,i} \boldsymbol{u}_g) =$$
$$\nabla \cdot (\rho_g D \varepsilon_g \nabla Y_{g,i}) + \delta \dot{m}_{i,chem}$$

(6)

Particles distribution function (O'Rourke and Snider, 2010):

$$\frac{df_p}{dt} + \frac{\partial(f_p \boldsymbol{u}_p)}{dx} + \frac{\partial(f_p \boldsymbol{A}_p)}{du_p} = \frac{f_D - f_p}{\tau_D}$$

(7)

Particles acceleration equation

$$\boldsymbol{A}_p = \frac{d\boldsymbol{u}_p}{dt} = D_p(\boldsymbol{u}_g - \boldsymbol{u}_p) - \frac{1}{\rho_p} \nabla p_g + \boldsymbol{g}$$
$$- \frac{1}{\varepsilon_p \rho_p} \nabla \tau_p + \boldsymbol{g} + \frac{\overline{\boldsymbol{u}}_p - \boldsymbol{u}_g}{\tau_D}$$

(8)

Drag model (Wen and Yu 1966)

$$D_p = C_D \frac{3}{8} \frac{\rho_g}{\rho_p} \frac{|\boldsymbol{u_g} - \boldsymbol{u_p}| \varepsilon_g^{-2.65}}{r_p}$$

(9)

$$C_D = \begin{cases} \frac{24}{Re}(1 + 0.15Re^{0.687}) & Re < 1000 \\ 0.44Re & \geq 1000 \end{cases}$$

(10)

$$Re = \frac{\rho_g |\boldsymbol{u_g} - \boldsymbol{u_p}|}{\mu_g} \quad and \quad r_p = \left(\frac{m_p}{\frac{4}{3}\pi\rho_p}\right)^{1/3}$$

(11)

The solid velocity is expressed as:

$$\frac{d\boldsymbol{x_s}}{dt} = u_p$$

(12)

Particles collision normal stress

$$\tau = \frac{P_p \varepsilon_p^\beta}{max[(\varepsilon_{cp} - \theta_p), \epsilon(1 - \varepsilon_p)]}$$

(13)

Particles volume fraction

$$\varepsilon_p = - \iiint f_p \frac{m_p}{\rho_p} dm_p d\boldsymbol{u_p} dT_p$$

(14)

Momentum transfer between phases

$$\boldsymbol{F} = - \iiint f_p \left\{ m_p \left[D_p(\boldsymbol{u_g} - \boldsymbol{u_p}) - \frac{\Delta p}{\rho_p} \right] + \boldsymbol{u_p} \frac{dm_p}{dt} \right\} dm_p d\boldsymbol{u_p} dT_p$$

(15)

Particles energy equation

$$C_V \frac{dT_p}{dt} = \frac{1}{m_p} \frac{\lambda_g Nu_{g,p}}{2r_p} A_p(T_g - T_p)$$

(16)

Conservative energy exchange term

$$S_h = \iiint f_D \left\{ m_p \left[D_p(\boldsymbol{u_p} - \boldsymbol{u_g})^2 - C_V \frac{dT_p}{dt} \right] - \frac{dm_p}{dt} \left[h_p + \frac{1}{2}(\boldsymbol{u_p} - \boldsymbol{u_g})^2 \right] dm_p d\boldsymbol{u_p} dT_p \right\}$$

(17)

Chemical reactions kinetics

$$k = A_o m_p^{C_1} T^{c2} exp\left(-\frac{E}{RT} + E_0\right)$$

(18)

T is the temperature of a particle gas film, obtained by averaging the particle temperature and the gas temperature.

3. GASIFIER DESCRIPTIONS

The aim of oxygen-blown gasifier is the production of a synthetic, nitrogen-free fuel gas (syngas) via coal steam gasification. The gasification chamber has a variable cross section area and is 3.5 m high. Figure 1 shows the geometrical model used in the simulations. Details of the experimental protocol are reported in Stendardo *et al.* (2016).

Below a brief description of this procedure is reported.

The gasifier can be fed approximately with 1.4 ton of anthracite/day (0.5 MWth) and it operates at 800 °C and 111460 Pa. The experimental campaign has been divided into five main consequentially steps:

1. *Gasifier heating up:* the reaction chamber is heated up to 500 °C via an auxiliary methane burner. During this step steam is produced to keep the piping warm enough, preventing any potential steam condensation during the injection in the gasification step.

2. *Bed material feeding*: when the temperature reaches 500 °C, olivine with a certain amount of coal is fed in order to build up the bed.

The flow rate of olivine is adjusted in order to keep a bed temperature in the range of 500–530 °C. When the temperature of the gasifier reaches the ignition temperature, heat released from coal combustion increases reaction chamber temperature, improving combustion efficiency;
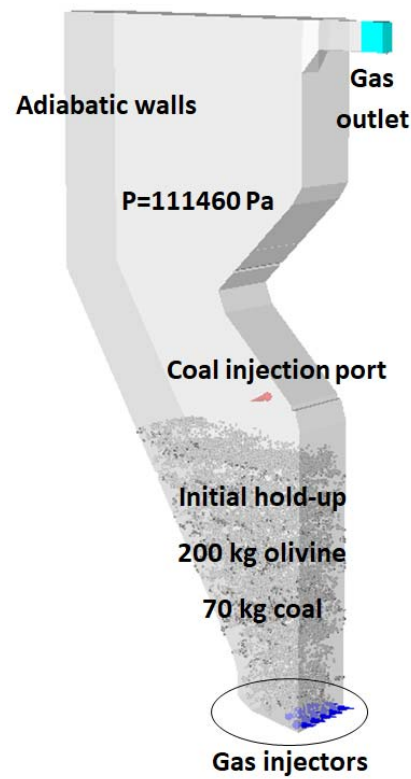

Fig. 1. Gasifier 3D model.

1. *Fluidization*: the particulate matter composed of olivine, ash and unburnt coal particles is fluidized by 120 kg/h of air, heated up to 200 °C in a heat exchanger by the flue gasses exiting the gasifier;

2. *Coal feeding:* coal feeding starts when the temperature of the gasifier is approximately 520 °C. The coal is fed via a gravity feeding system at a flow rate of 8 kg/h; the auxiliary methane burner is turned off and coal burns in the fluidizing air;

3. *Gasification*: when the temperature reaches 700 °C the air flow rate is progressively decreased while both the flow rate of oxygen and steam are increased. Oxygen coming from a cryogenic vessel is heated up to 100 °C via an electric heat exchanger Simultaneously, the feeding rate of coal is increased up to 50-60 kg/h. The temperature

during the gasification test is approximately 800 °C. The particle bed is directly heated by the thermal energy released by the combustion of part of the coal and pyrolysis product, supplying the necessary heat for the endothermic gasification reactions.

Syngas is then cleaned of fine matter in a cyclone and cooled down to 600 °C in a heat exchanger used to heat up the gasifying medium. The cooled syngas is then
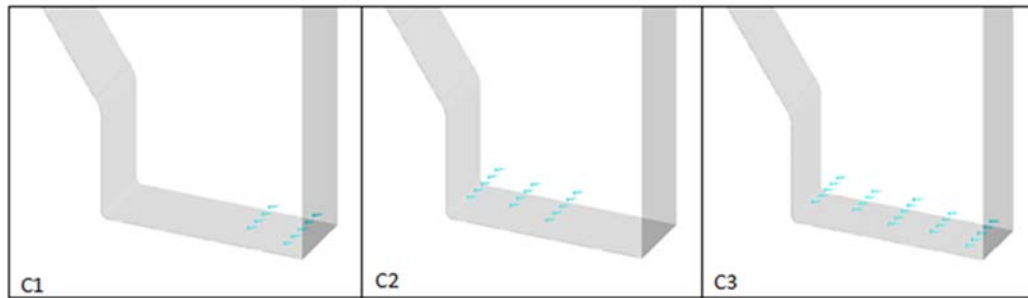

Fig. 2. Fluidizing gas injectors position.

scrubbed in a three-step spray water system and burnt with air in a flare. The gasifier injection system is composed of 23 staggered injectors (Fig. 2), placed at the bottom of the reactor, protected by metal elements (Fig. 3), which help to prevent possible obstructions caused by a flow of the particles.

4. RESULTS

A parametric analysis with regards to the injection strategy has been carried out and the main results have been reported in this section. The fluidization analysis has been conducted for the three possible injection configurations (Fig. 2) and for different fluidizing gas mass flow rates. In the configuration C1 only the 9 injectors placed near the right wall are fed. In the configuration C2 the other 14 injectors are fed. In the configuration C3 all the injectors are fed at the same time. Since the overall mass flow is distributed among the injectors, the configuration C1 presents higher injection velocity, while the configuration C3 presents the lower ones. The complete set of simulations is reported in Table 1. In Barracuda® fluid injectors are treated as point injections since the minimum mesh cells dimension is limited by particles size, i.e. a cell must be large enough to contain a sufficient number of particles. Then several simulations have been carried out, with the aim to calculate a correct injection velocity for each mass flow rate used for the CPFD simulations. These series of simulations have been performed by Ansys-Fluent® software, using a tetrahedral computational grid. As it is clearly reported by Fig. 3, the flow exiting from the injector is deviated and guided by the cover elements toward the particles bed. The insertion angle is determined by the elements covering the injection gas, while the velocity magnitude has been calculated averaging the velocity distribution on the effective cross section surface.

In the non-reacting fluidization simulations the initial bed is composed of 200 kg of olivine and 70 kg of coal, with size distribution reported in Fig. 5 and 6 and the initial temperature is 800 °C. The fresh coal injection has been neglected here. A small amount of particles (5 kg) acting as tracer and

having the same characteristics of the coal has been added as a thin layer on the top of the bed, to study the mixing effectiveness of the different configurations. A pressure condition has been set at the reactor outlet.

Table 1 Non-reactive simulations summary.

	Gas mass flow rate (kg/h)		
	Low	Medium	High
C1	75	96	-
C2	75	96	-
C3	75	96	144

The model simulates the gasifier under adiabatic condition while the operating pressure is 111460 Pa. The fluidizing gas mixture, injected as mass flow point injections through the system described above, is composed of 50 % of oxygen and 50 % of water vapor by mass at 400 °C. The computational Cartesian grid (Fig. 4) is made of 485000 uniform cells and the grid is automatically adapted at the boundary walls. The numerical grid does not take into account the cyclone. A schematic of the boundary conditions adopted is reported in Fig. 1. The unsteady non-reactive simulations have been carried out for few seconds of simulation time, until no significant variations have been observed in the tracer mixing. The solver auto adjusts the time-step, up to a maximum imposed limit (0.01 s). No validation has been conducted for the cold-flow analysis due to the absence of measured data.
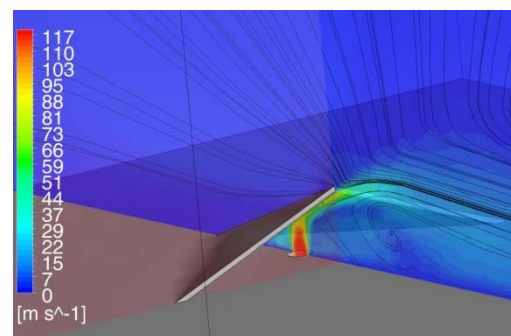

Fig. 3. Injector simulation. Velocity map.

Regarding the influence of the active nozzles and the mass flow rates of the fluidizing gas in all the

investigated cases, it is evident that the mass flow rates ensure a bubbling fluidization regime avoiding the entrainment of solid particles (Figs. 7-9). Furthermore, when the nozzles are activated in the C1 and C2 configurations, the gaseous flow exhibits preferential paths that do not allow the gas contact with the whole solid mass. This is evident in particular in the case C1, for which the gas flows completely along the wall. In this case for the higher mass flow rate, there is a consistent splashing of the lighter particles on the walls of the gasifier. The C3 configuration is the only one which guarantees a more effective contact of the gas with the solid mass and a better bubbling fluidization regime, although the general lower injection velocity for the same mass flow. Due to the geometrical configuration of the gasifier and to the direction of the nozzles, the part of the bed adjacent to the leaning wall is not crossed by the gas flow.
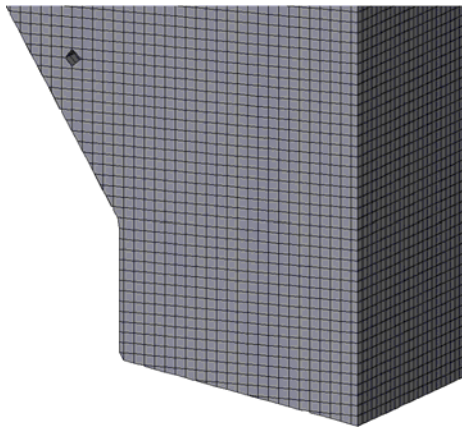
Fig. 4. Fluidization cases mesh detail.

This is more apparent from the tracer position (see right panel of Figs. 7-9), which mixes within the bed mainly along the vertical wall in the C1 cases, while is more distributed for the C2 and C3 cases. Only the C3 configuration was further simulated at 144 kg/h, since in the other ones the discharge velocity from the nozzles would have been extremely high.
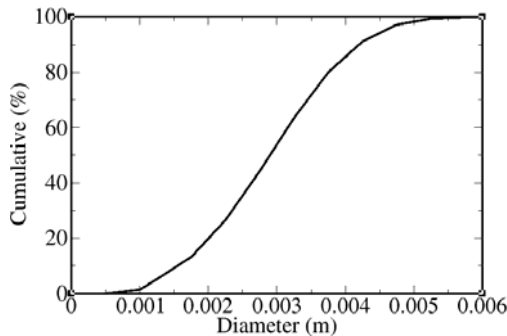

Fig. 5. Coal particles size distribution.

Gasification is a complex process involving a series of reactions which are currently under investigation in the scientific literature. The kinetic equations adopted in this work are reported below along with the related chemical reactions. This set of equations have been implemented in the Barracuda® code, with the reaction rate r expressed in mol/(m³s).
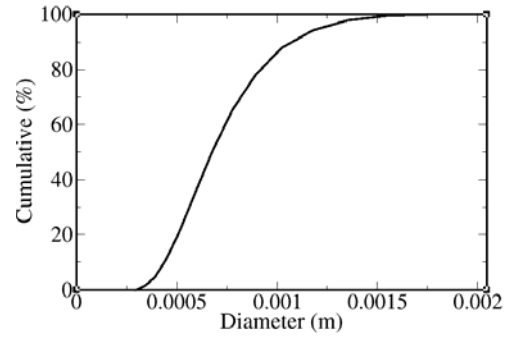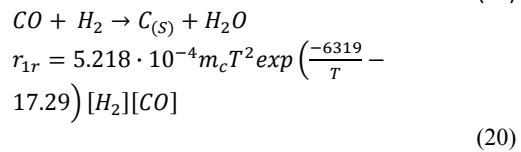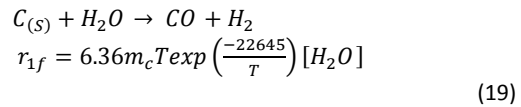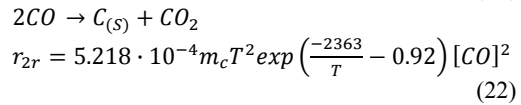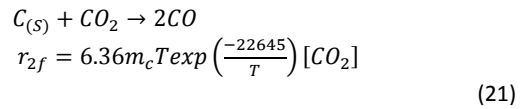

Fig. 6. Olivine particles size distribution.
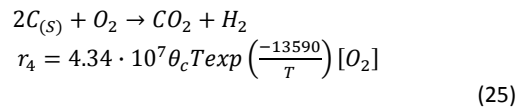
1) Steam Gasification (Syamlal and Bisset 1992):

$$C_{(S)} + H_2O \rightarrow CO + H_2$$
$$r_{1f} = 6.36 m_c T exp\left(\frac{-22645}{T}\right)[H_2O] \tag{19}$$

$$CO + H_2 \rightarrow C_{(S)} + H_2O$$
$$r_{1r} = 5.218 \cdot 10^{-4} m_c T^2 exp\left(\frac{-6319}{T} - 17.29\right)[H_2][CO] \tag{20}$$

2) CO_2 Gasification (Syamlal and Bisset 1992):

$$C_{(S)} + CO_2 \rightarrow 2CO$$
$$r_{2f} = 6.36 m_c T exp\left(\frac{-22645}{T}\right)[CO_2] \tag{21}$$

$$2CO \rightarrow C_{(S)} + CO_2$$
$$r_{2r} = 5.218 \cdot 10^{-4} m_c T^2 exp\left(\frac{-2363}{T} - 0.92\right)[CO]^2 \tag{22}$$

3) Methanation (Syamlal and Bisset 1992):

$$0.5 C_{(S)} + H_2 \rightarrow 0.5 CH_4$$
$$r_{3f} = 6.838 \cdot 10^{-3} m_c T exp\left(\frac{-8078}{T} - 7.087\right)[H_2] \tag{23}$$

$$0.5 CH_4 \rightarrow 0.5 C_{(S)} + H_2$$
$$r_{3r} = 0.755 m_c T^{0.5} T exp\left(\frac{-13578}{T} - 0.372\right)[CH_4]^{0.5} \tag{24}$$
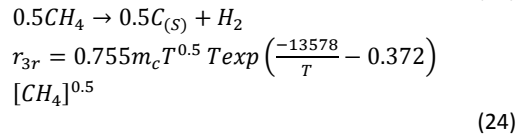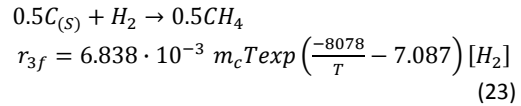
4) Combustion (Yoon *et al.* 1978):

$$2C_{(S)} + O_2 \rightarrow CO_2 + H_2$$
$$r_4 = 4.34 \cdot 10^7 \theta_c T exp\left(\frac{-13590}{T}\right)[O_2] \tag{25}$$

5) Water gas-shift (Bustamante *et al.* 2004, 2005):

$$CO + H_2O \rightarrow CO_2 + H_2$$
$$r_{5f} = 7.68 \cdot 10^{10} exp\left(\frac{-36640}{T}\right)[CO]^{0.5}[H_2O] \tag{26}$$

$$CO_2 + H_2 \rightarrow CO + H_2O$$
$$r_{5r} = 6.4 \cdot 10^9 exp\left(\frac{-39260}{T}\right)[H_2]^{0.5}[CO_2] \tag{27}$$
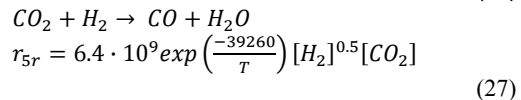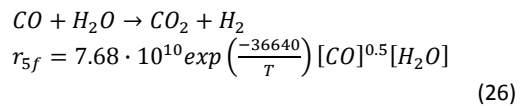
In order to contain the computational cost, a coarser mesh has been adopted for the gasification analysis. The initial and boundary conditions are the same for the non-reactive simulations in the C1 configuration, for 48 kg/h of fluidizing gas mass flow rate (50 % O_2, 50 % H_2O by mass), at 150 °C. In addition, a fresh coal mass flow rate of 45 kg/h is

fed to the reactor from a discharge port located above the bed and is treated as mass flow point injection (Fig. 1). The high-rank anthracite coal used is composed of 89.3 % of char, 1.7 % of water and 9 % of ash, water vapor is then the only gaseous species released in the model as a function of temperature, according to:

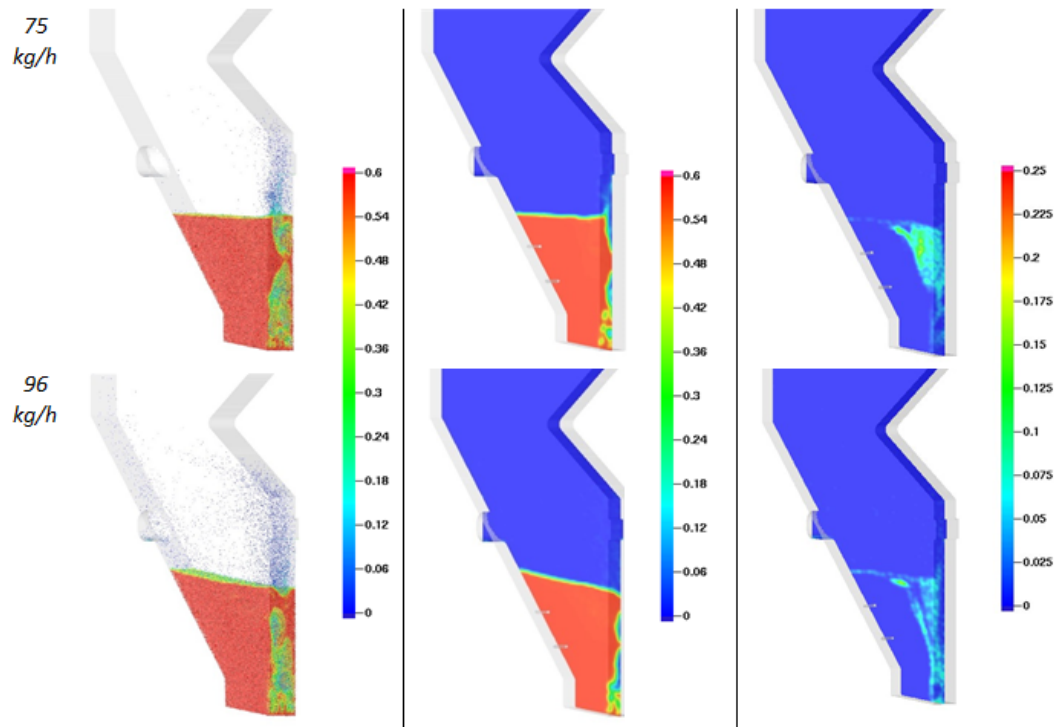$$\dot{m} = 0.05 T_p e^{-5500/T_p} \, \text{kg/s} \qquad (28)$$

Fig. 7. Particles mass fraction (left), particles volume fraction (middle) and tracer volume fraction (right), case C1.
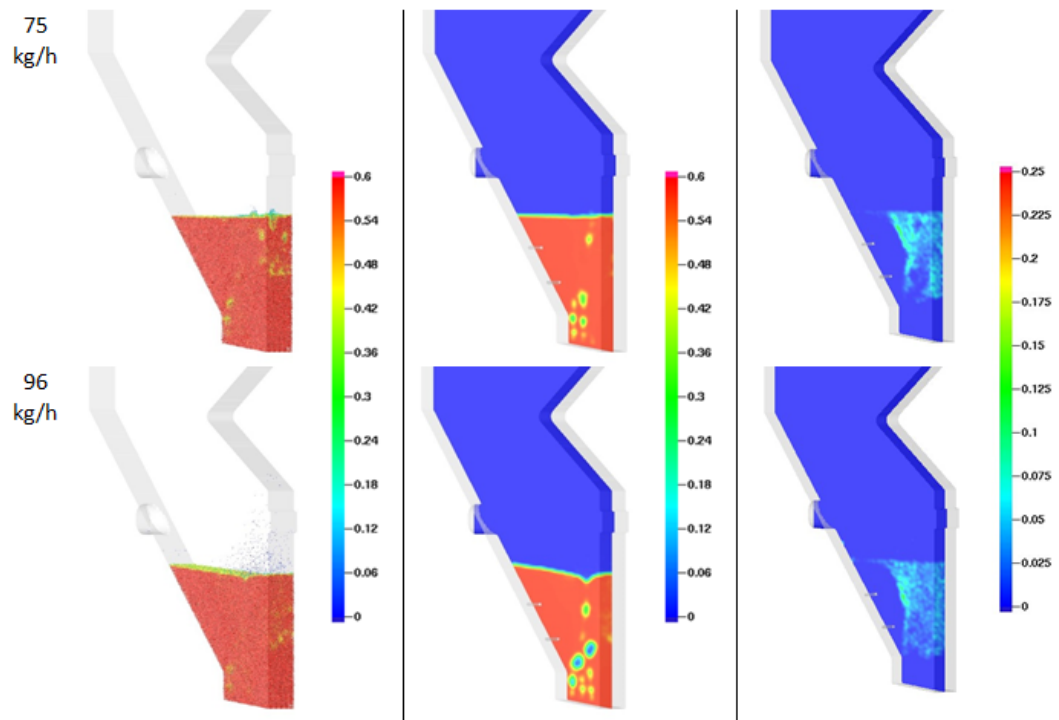
Fig. 8. Particles mass fraction (left), particles volume fraction (middle) and tracer volume fraction (right), case C2.
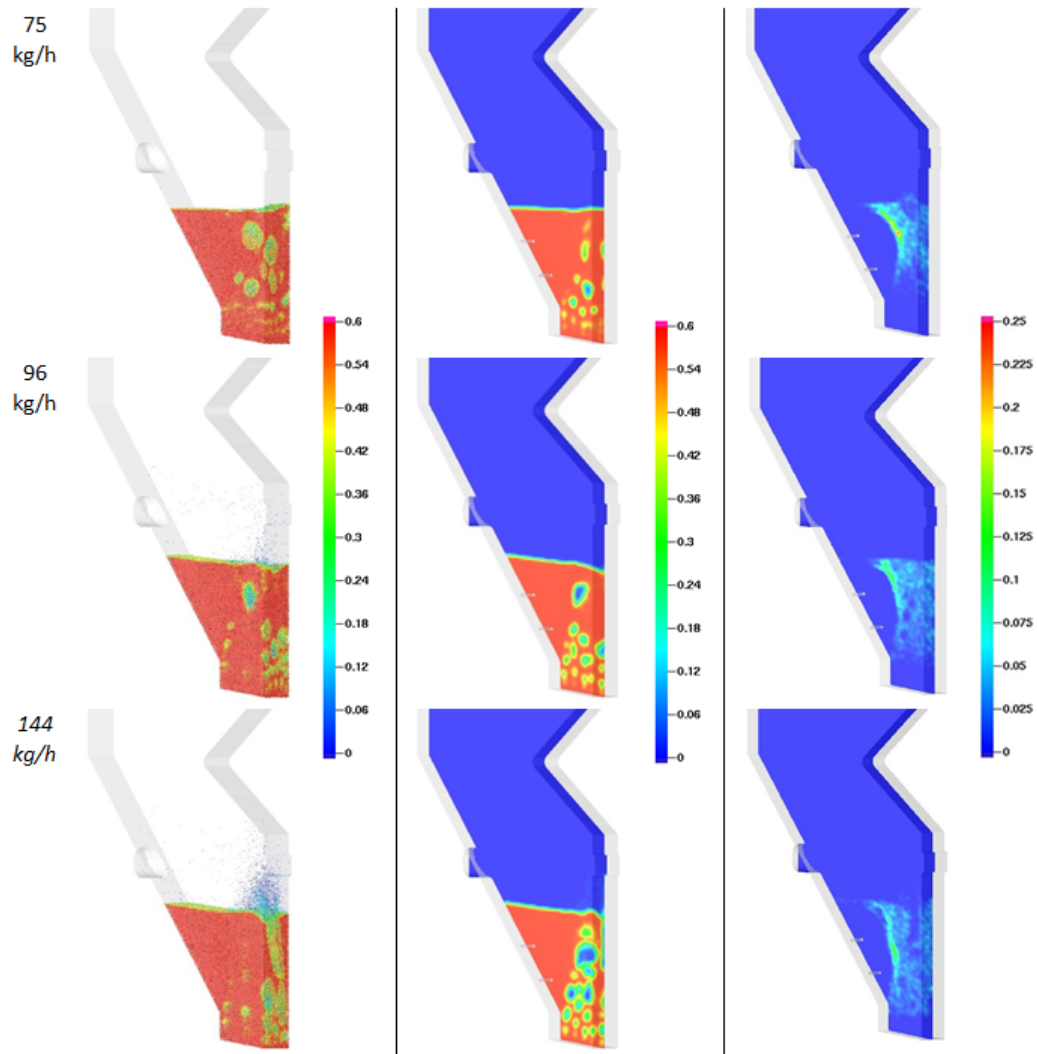
Fig. 9. Particles mass fraction (left), particles volume fraction (middle) and tracer volume fraction (right), case C3.

Then there are no reactive volatiles species considered in the model. The unsteady simulation reaches a steady state after several minutes of simulation time for what regards the output gas composition and temperature, starting from an initial bed temperature close to the regime temperature. As it is clear from the Fig. 10, as the time proceeds, the coal, which is lighter than olivine, stratifies in the upper part of the bed also because it is consumed by reactions in the lower part. The output gas composition obtained from the simulation is comparable with the experimental data (Fig. 12). The deviations between calculated and measured data are -12.5 %, 12.5 % and 0 %, for CO, CO_2 and H_2, respectively. Figure 11 reports the oxygen distribution inside the gasifier. It is clear that oxygen is consumed by the combustion reaction among the first layers of the particle bed.

5. CONCLUSIONS

In this paper, the coal oxygen-blown gasifier of the ZECOMIX research infrastructure has been studied and simulated by means of the CPFD approach.
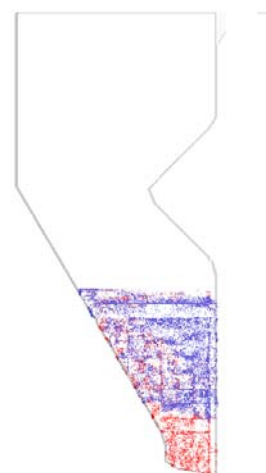

Fig. 10. Coal (blue) and olivine (red) particles distribution.

The proposed method has resulted as a powerful and efficient approach for fluidized bed simulation where a huge number of particles has to be taken into account.

In the non-reacting fluidization cases, the different injectors configuration have been evaluated with respect to bubbling and mixing effects.

In the reacting cases, the evaluation of the syngas composition has resulted in a good agreement with the available experimental data collected in the ZECOMIX research infrastructure.

The research infrastructure is composed of other types of fluid-bed reactors, such as the calciner and the carbonator, which can therefore enjoy the same computational advantages offered by the numerical approach used in this work, and which are currently being studied.
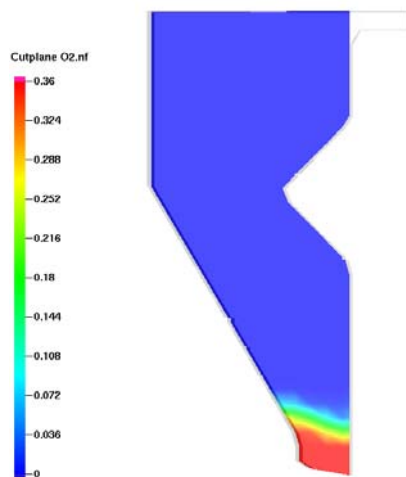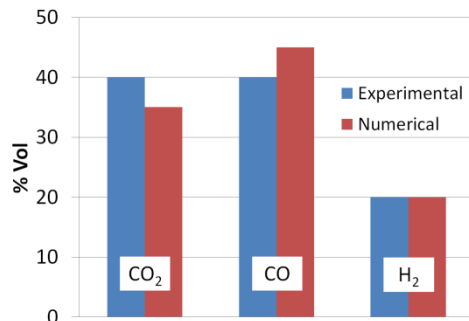

Fig. 11. Oxygen volumetric concentration.

Fig. 12. Experimental and numerical output syngas composition comparison.

ACKNOWLEDGEMENTS

REFERENCES

Andrews, J., P. J., O'Rourke (1996). The multiphase particle-in-cell (Mp-Pic) method for dense particulate flows. *International Journal of Multiphase Flow*, 22, 379-402.

Bustamante, F., R. M., Enick, A. V., Cugini, R. P., Killmeyer, B.H., Howard, K.S., Rothenberger, M.V., Ciocco, B.D., Morreale, S., Chattopadhyay, S., Shi (2004). High-temperature kinetics of the homogeneous reverse water–gas shift reaction. *AIChE Journal*, 50, 1028–1041.

Bustamante, F., R. M., Enick, R. P., Killmeyer, B.H.,Howard, K.S., Rothenberger, A.V., Cugini, B.D., M.V., Morreale, Ciocco (2005). Uncatalyzed and wall-catalyzed forward water–gas shift reaction kinetics. *AIChE Journal*, 51, 1440–1454.

Deen, N. G., M., Van Sint Annaland, M. A., Van der Hoef, J.A.M., Kuipers (2007). Review of discrete particle modeling of fluidized beds. *Chemical Engineering Science*, 62, 28–44.

Gidaspow, D. (1994). *Multiphase Flow and fluidization: continuum and kinetic theory descriptions*. American Press, Boston.

Gidaspow, D., J., Jung, R.K., Singh (2004). Hydrodynamics of fluidization using kinetic theory: an emerging paradigm: 2002 Flour-Daniel lecture. *Powder Technology*, 148, 123–141.

Harris, S. E., D. G., Crighton (1994). Solitons, solitary waves and voidage disturbances in gas-fluidized beds. *Journal of Fluid Mechanics*, 266, 243–276.

Karimipour, S., T., Pugsley (2012). Application of the particle in cell approach for the simulation of bubbling fluidized beds of Geldart A particles. *Powder Technology*, 220, 63–69.

Kraft, S., M., Kuba, F., Kirnbauer, K., Bosch, H., Hofbauer (2016). Optimization of a 50 MW bubbling fluidized bed biomass combustion chamber by means of computational particle fluid dynamics. *Biomass and Bioenergy*, 89, 31-39.

Lettieri, P., L., Mazzei (2009). Challenges and issues on the CFD modeling of fluidized beds: a review. *Journal of Computational Multiphase Flows*, 1, 83–131.

Liang, Y., Y., Zhang, T., Li, C., Lu (2014). A critical validation study on CPFD model in simulating gas–solid bubbling fluidized beds. *Powder Technology*, 263, 121–134.

Liu, H., R. J., Cattolica, R., Seiser, C., Liao (2015). Three-dimensional full-loop simulation of a dual fluidized-bed biomass Gasifier. *Applied Energy*, 160, 489–501.

O'Rourke, P. J., D. M., Snider (2010). An improved collision damping time for MP-PIC

calculations of dense particle flow with applications to polydisper sedimenting bed sand colliding particle jets. *Chemical Engineering Science*, 65, 6014–6028.

O'Rourke, P. J., P., Zhao, D., Snider (2009). A model for collisional exchange in gas/liquid/solid fluidized beds. *Chemical Engineering Science*, 64, 1784–1797.

Ponti, G., F., Palombi, D., Abate, F., Ambrosino, G., Aprea, T., Bastianelli, F., Beone, R., Bertini, Bracco, G., Caporicci, M., Calosso, B., Chinnici, M., Colavincenzo, A., Cucurullo, A., Dangelo, P., De Rosa, M., De Michele, P., Funel, A., Furini, G., Giammattei, D., Giusepponi, S., Guadagni, R., Guarnieri, G., Italiano, A., Magagnino, S., Mariano, A., Mencuccini, G., Mercuri, C., Migliori, S., Ornelli, P., Pecoraro, S., Perozziello, A., Pierattini, S., Podda, S., Poggi, F., Quintiliani, A., Rocchi, A., Scio, C., Simoni, F., Vita, A. (2014). The role of medium size facilities in the HPC ecosystem: the case of the new CRESCO4 cluster integrated in the ENEAGRID infrastructure. In *Proceedings of the 2014 International Conference on High Performance Computing and Simulation, HPCS 2014*, art. no. 6903807, 1030-1033.

Smagorinsky. J. (1963). General Circulation Experiments with the Primitive Equations. I. The Basic Experiment. *Monthly Weather Review*, 91, 99-164.

Snider, D., S., Banerjee (2010). Heterogeneous gas chemistry in the CPFD Eulerian–Lagrangian numerical scheme (ozone decomposition). *Powder Technology*, 199, 100–106.

Snider, D. M. (2001). An incompressible three-dimensional multiphase particle-in-cell model for dense particle flows. *Journal of Computational Physics*, 170, 523–549.

Snider, D. M., S. M., Clark, P. J. O'Rourke (2011). Eulerian–Lagrangian method for threedimensional thermal reacting flow with application to coal gasifiers. *Chemical Engineering Science*, 66, 1285–1295.

Stendardo S., P. U., Foscolo, M., Nobili, S., Scaccia (2016). High quality syngas production via steam-oxygen blown bubbling fluidised bed gasifier. *Energy*, 103, 697-708.

Syamlal, M., L. A., Bisset, (1992). *METC gasifier advanced simulation (MGAS) model*. DOE/METC–92/4108, DE92 001111.

Thapa, R. K., A., Frohner, G., Tondl, C., Pfeifer, B.M., Halvorsen, (2016). Circulating fluidized bed combustion reactor: computational particle fluid dynamic model validation and gas feed position optimization. *Computers and Chemical Engineering*, 92, 180–188.

Thapa, R. K., C., Pfeifer, B. M., Halvorsen, (2014). Modeling of reaction kinetics in bubbling fluidized bed biomass gasification reactor. *Int. Journal of Energy and Environment*, 5, 35-44.

Wang, J. (2009). A review of Eulerian simulation of Geldart A particles in gas-fluidized beds. *Industrial and Engineering Chemistry Research*, 48, 5567–5577.

Wang, J., van der Hoef, M. A., Kuipers, J. A. M. (2013). Comparison of two-fluid and discrete particle modeling of dense gas-particle flows in gas-fluidized beds. *Chemical Engineering and Technology*, 85, 290–298.

Wen, C., Y., Yu (1966). Mechanics of fluidization. In *Chemical Engineering Progress Symposium*. Ser., 62, 100–111.

Yoon, H., J., Wei, M. M., Denn (1978). A model for moving-bed coal gasification reactors. *AIChE Journal*, 24, 885–903.